



This discussion paper is/has been under review for the journal Atmospheric Measurement Techniques (AMT). Please refer to the corresponding final paper in AMT if available.

# CHAMP climate data based on inversion of monthly average bending angles

J. Danzer<sup>1</sup>, H. Gleisner<sup>2</sup>, and S. B. Healy<sup>3</sup>

<sup>1</sup>Wegener Center for Climate and Global Change (WEGC), University of Graz, Graz, Austria

<sup>2</sup>Danish Meteorological Institute (DMI), Copenhagen, Denmark

<sup>3</sup>European Centre for Medium-range Weather Forecasts (ECMWF), Reading, UK

Received: 10 July 2014 – Accepted: 14 July 2014 – Published: 29 July 2014

Correspondence to: J. Danzer (julia.danzer@uni-graz.at)

Published by Copernicus Publications on behalf of the European Geosciences Union.

## Average bending angle approach

J. Danzer et al.

Title Page

Abstract

Introduction

Conclusions

References

Tables

Figures



Back

Close

Full Screen / Esc

Printer-friendly Version

Interactive Discussion



## Abstract

GNSS Radio Occultation (RO) refractivity climatologies for the stratosphere can be obtained from the Abel inversion of monthly average bending-angle profiles. The averaging of large numbers of profiles suppresses random noise and this, in combination with simple exponential extrapolation above an altitude of 80 km, circumvents the need for a “statistical optimization” step in the processing. Using data from the US-Taiwanese COSMIC mission, which provides ~ 1500–2000 occultations per day, it has been shown that this Average-Profile Inversion (API) technique provides a robust method for generating stratospheric refractivity climatologies.

Prior to the launch of COSMIC in mid-2006, the data records rely on data from the CHAMP mission. In order to exploit the full range of available RO data, the usage of CHAMP data is also required. CHAMP only provided ~ 200 profiles per day, and the measurements were noisier than COSMIC. As a consequence, the main research question in this study was to see if the average bending angle approach is also applicable to CHAMP data.

Different methods for suppression of random noise – statistical and through data quality pre-screening – were tested. The API retrievals were compared with the more conventional approach of averaging individual refractivity profiles, produced with the implementation of statistical optimization used in the EUMETSAT Radio Occultation Meteorology Satellite Application Facility (ROM SAF) operational processing.

In this study it is demonstrated that the API retrieval technique works well for CHAMP data, enabling the generation of long-term stratospheric RO climate data records from August 2001 and onward. The resulting CHAMP refractivity climatologies are found to be practically identical to the standard retrieval at the DMI below altitudes of 35 km. Between 35 km to 50 km the differences between the two retrieval methods started to increase, showing largest differences at high latitudes and high altitudes. Furthermore, in the winter hemisphere high latitude region, the biases relative to ECMWF were generally smaller for the new approach than for the standard retrieval.

AMTD

7, 7811–7835, 2014

## Average bending angle approach

J. Danzer et al.

Title Page

Abstract

Introduction

Conclusions

References

Tables

Figures



Back

Close

Full Screen / Esc

Printer-friendly Version

Interactive Discussion



# 1 Introduction

GNSS radio occultation (GNSS-RO) receivers onboard low-Earth orbit (LEO) satellites have provided a nearly continuous global data record on the state of the atmosphere since the launch of the German CHAMP (CHALLENGING Mini-Satellite Payload) satellite in 2001. During its 7 year lifetime CHAMP on average provided around 200 occultations per day. With the launch of the six-satellite constellation FORMOSAT-3/COSMIC (henceforth referred to as COSMIC) (Constellation Observing System for Meteorology, Ionosphere, and Climate) in mid-2006, the number of occultations per day increased by an order of magnitude to more than 2000. A number of research satellites add further to the RO data records, and in late 2006 the first in a planned series of European polar-orbiting Metop satellites, carrying RO instruments, became operational.

GNSS-RO it is likely to play an increasingly important role in climate research and climate monitoring, particularly for the upper troposphere and stratosphere. The GNSS-RO data provide accurate geophysical information with a high vertical resolution at altitudes from around 5 km to 40 km. A decisive advantage compared to other measurement techniques is that RO data from different instruments and missions can be combined without inter-calibration of the data records. This is a consequence of the fact that the primary observable is phase shifts, or time differences, rather than radiances.

The observed phase shifts of the GNSS carrier wave during an occultation are processed to ray bending angles without the explicit use of any a priori information. However, the retrieval of more traditional atmospheric variables from the measurements requires the extrapolation of the bending angle profile to infinity using an a priori model of bending angles. The first step in that retrieval is the computation of a refractivity profile from the bending angle profile using an Abel transformation, where extrapolation to infinity is required due to the upper limit in the Abel integral (Eq. 1). The observed bending angle profile is limited in altitude by a decreasing signal-to-noise ratio – the observed bending angle values fall off exponentially while the dominating measurement errors are relatively constant with height. For the current generation of RO instruments,

## AMTD

7, 7811–7835, 2014

### Average bending angle approach

J. Danzer et al.

Title Page

Abstract

Introduction

Conclusions

References

Tables

Figures



Back

Close

Full Screen / Esc

Printer-friendly Version

Interactive Discussion



## Average bending angle approach

J. Danzer et al.

Title Page

Abstract

Introduction

Conclusions

References

Tables

Figures

◀

▶

◀

▶

Back

Close

Full Screen / Esc

Printer-friendly Version

Interactive Discussion



and the operationally used processing schemes, the observed bending angle values and the errors are of roughly the same magnitude near  $\sim 60$  km. Above that, the errors are larger than the observed bending angles.

To handle the exponentially decreasing signal-to-noise ratios, the extrapolation step and merging with the a priori bending angle information is often combined with a smoothing of the retrieved bending angles over an extended vertical interval, usually above  $\sim 40$  km. This processing step is referred to as “statistical optimization” (SO). The “optimized” bending angle profiles are then used to retrieve refractivity profiles, and from that profiles of temperature, geopotential height and pressure are derived. Different approaches to the statistical optimization have been described in some detail by, e.g., Gorbunov (2002); Lohmann (2005); Gobiet and Kirchengast (2004). Specific details of implementations at various GNSS-RO processing centres have been described by Ho et al. (2009, 2012), while the SO scheme used at the ROM SAF (Radio Occultation Meteorology Satellite Application Facility) is outlined in Lauritsen et al. (2011). The errors introduced by the statistical optimization are difficult to characterise and quantify. Furthermore, recent studies within the *ROtrends* working group have shown that the upper-level bending angle initialization may be a source of structural uncertainties for the climate data products (Ho et al., 2012; Steiner et al., 2013). The different methods and background information used in the SO of processing centers, leads to differences in the climate data products mainly above 25 km.

Climatologies of the geophysical parameters, e.g zonally gridded monthly means, are commonly derived by binning and averaging the individually retrieved, statistically optimized, profiles. However, recent studies have used an alternative processing approach, which circumvents the statistical optimization step, and has a clear – but weak – dependency on the assumed a priori. Ao et al. (2012) and Gleisner and Healy (2013) independently described the use of averaged bending angles, instead of individual profiles. In this Average Profile Inversion (API) technique, the required suppression of random noise is obtained through averaging a large number of profiles, rather than smoothing and merging with a background. The feasibility of this approach was demonstrated with

**Average bending angle approach**

J. Danzer et al.

Title Page

Abstract

Introduction

Conclusions

References

Tables

Figures



Back

Close

Full Screen / Esc

Printer-friendly Version

Interactive Discussion



COSMIC data, which provides 1500–2000 profiles per day. Furthermore, preliminary investigations also showed that the method is relatively robust to a large reduction of data numbers – a random removal of 85 % of the data gave very small differences of the mean refractivities below 40 km (Gleisner and Healy, 2013). However, it remained unclear whether the API approach could be applied to the period from 2001–2006 when only CHAMP was available. CHAMP only provided  $\sim 200$  profiles per day, and they were considerably noisier than the COSMIC and Metop data available from the latter half of 2006 and onward. Any method used to generate RO climate data records must be able to handle this situation. Therefore, the present study investigates the applicability of the API method during the CHAMP era. The suppression of noise by averaging, and the role of quality control procedures, are also investigated.

Furthermore, it has been shown that the bending angle initialization used until recently in the standard retrieval scheme at the DMI (Danish Meteorological Institute), which is the MSIS climatology (Mass Spectrometer and Incoherent Scatter Radar), may exhibit biases during winter conditions at high altitudes and high latitudes (Steiner et al., 2013). Hence, one of the research questions is if the initialization can be improved for climate data using the new average bending angle approach. Currently, at the level of single refractivity profiles, the DMI is addressing this existing limitations by algorithm improvements and by using the so-called BAROCLIM spectral model (Bending Angle Radio Occultation Climatology) as their a priori information (Foelsche and Scherllin-Pirscher, 2011; Scherllin-Pirscher, 2013) for the SO. In this study we concentrate especially on the high latitude and altitude region, comparing the new averaging approach to the standard approach.

The data used in this study are described in Sect. 2.1. Section 2.2 describes the processing of the data to refractivity. An analysis of averaged bending angles is given in Sect. 3, while the main results of API processed bending angles are presented in Sect. 4. The discussion and conclusions are given in Sect. 5.

## 2 Data sets and method

### 2.1 Data sets

The study focuses on occultation events observed by the CHAMP single satellite mission from September 2001 until September 2008. At the UCAR/CDAAC database (University Corporation for Atmospheric Research/COSMIC Data Analysis and Archive Center) excess phase profiles and precise orbit information were retrieved, and further processed into bending angle and refractivity profiles at the ROM SAF, which is a RO processing center under EUMETSAT (European Organisation for the Exploitation of Meteorological Satellites), hosted by the DMI, using the ROPP (Radio Occultation Processing Package) software as their retrieval package.

In this study, the bending angle and refractivity profiles were analyzed on a monthly basis for  $10^\circ$  zonal bins, leading to between about 3500 to 5500 profiles per month in case of CHAMP data, and about 50 000 to 65 000 profiles per month for COSMIC data, after several steps of quality screening (Gorbunov et al., 2006).

Furthermore co-located ECMWF (European Centre for Medium-Range Weather Forecasts) refractivity and bending angle profiles from ECMWF analysis data were studied on  $10^\circ$  latitudinal bins and used as a reference for the monthly mean profiles. The used analysis data fields were studied on a T42L91 resolution, since the T42 horizontal resolution matches the resolution of RO data ( $\sim 300$  km). Until January 2006 they are given on 60 vertical levels (L60), after that the ECMWF switched to 91 vertical levels (L91). Furthermore, in December 2006 the ECMWF started to assimilate GPS RO data into the analysis fields.

### 2.2 Method

The production of geophysical parameters from GNSS RO measurements requires a retrieval chain described in detail by Kursinski et al. (1997). In the retrieval an Abel

Title Page

Abstract

Introduction

Conclusions

References

Tables

Figures



Back

Close

Full Screen / Esc

Printer-friendly Version

Interactive Discussion



transformation occurs, relating the refractive index  $n$  to the bending angle  $\alpha$ , through,

$$\ln n(x) = \frac{1}{\pi} \int_x^\infty \frac{\alpha(a)}{\sqrt{a^2 - x^2}} da \quad (1)$$

where  $a$  is the impact parameter and  $x = nr$ , with  $r$  being the radius of a point on the ray path. The integral over infinity poses a problem, since observational data has a limit in altitude to about 80 km. Hence an extrapolation to infinity becomes necessary. Furthermore the measurement noise grows in magnitude with increasing altitude. One widely used approach is to replace or merge the noisy observed bending angles with bending angles from a climatological model, often in combination with more or less complex smoothing filters. This is referred to as statistical optimization (SO), where a statistically optimized bending angle is obtained, i.e.,

$$\alpha = \alpha_b + \mathbf{K}(\alpha_O - \alpha_b) \quad (2)$$

yielding the optimized bending angle  $\alpha$ .  $\alpha_O$  and  $\alpha_b$  are the observed and the background bending angle, respectively.  $\mathbf{K}$  is the gain matrix, which can be written in terms of error covariance matrices for the observed and background bending angle profiles. Using the statistically optimized bending angle for the Abel transformation, refractivity profiles can be calculated. From refractivity other geophysical variables, such as density, pressure, temperature, are retrieved (for a more elaborated description see, e.g. Kursinski et al., 1997). When comparing the results of different processing centers, discrepancies in the atmospheric parameters arise mainly through the choice of the gain matrix and the background information (Ho et al., 2012; Steiner et al., 2013).

One of the most widely used sources of a priori background information has been the MSIS climatology. Until recently, this was also the standard at DMI. In this study it is used in an SO scheme based on Optimal Linear Combination (OLC) devised by Gorbunov (2002). It has been pointed out by, e.g., Gobiet and Kirchengast (2004) and Foelsche et al. (2008) that the use of MSIS climatology as a priori may cause problems

## Average bending angle approach

J. Danzer et al.

Title Page

Abstract

Introduction

Conclusions

References

Tables

Figures

◀

▶

◀

▶

Back

Close

Full Screen / Esc

Printer-friendly Version

Interactive Discussion



at high latitudes and high altitudes, particularly during winter. There may be no adequate profile in MSIS that fits the very cold conditions, and the best fitting profiles may simply be too warm.

In this study zonal monthly mean bending angle climatologies were primarily built and secondly, forwarded through the Abel transformation, to obtain zonal monthly refractivity climatologies (Ao et al., 2012; Gleisner and Healy, 2013). The averaged bending angle CHAMP data were used up to an altitude of 80 km. Above that an extrapolation of the averaged bending angle profiles to infinity was still necessary, due to the upper boundary of the Abel integral, see Eq. (1). An exponential extrapolation with a constant scale height of 7.5 km was used as in Gleisner and Healy (2013). Furthermore, the sensitivity at the assumed scale height was tested, and it had little impact below 40 km.

### 3 CHAMP bending angle averages

As a primary investigation, monthly average CHAMP bending angles within 10° latitude bins were built analog to the average COSMIC bending angles studied in Gleisner and Healy (2013). Figure 1 shows differences between the CHAMP average bending angles and ECMWF bending angles similarly constructed from co-located ECMWF profiles, using means and medians, respectively, and with/without the extra quality control described in Sect. 3.1. Below 50 km, errors resulting from ionospheric residuals, instrumental errors and neutral-atmosphere variability are suppressed due to averaging over many profiles within a bin and the mean value is a smoother estimate compared to the median value. Above that, the mean bending angle profiles show large-scale wiggles (Fig. 1a), leading to differences to the reference profile larger than  $\pm 2 \mu\text{rad}$ . The median bending angle profiles do not show such large-scale variations, however they suffer from small-scale variations which recommends the mean instead of the median bending angle as an average estimate below altitudes of about 50 km.

## Average bending angle approach

J. Danzer et al.

Title Page

Abstract

Introduction

Conclusions

References

Tables

Figures



Back

Close

Full Screen / Esc

Printer-friendly Version

Interactive Discussion



### 3.1 Bending angle quality control

In the processing from raw data to single bending angle profiles the DMI uses several screening steps in their quality control, in which data is partly or totally rejected (Gorbunov et al., 2006). However, regarding the increased noise in the usage of CHAMP satellite data compared to COSMIC satellite data, we decided to investigate the single bending angle profiles contributing to the monthly mean zonal bending angle estimates, more thoroughly.

The l.h.s. of Fig. 2 shows for an example zonal bin at mean latitude  $5^\circ$  all single profiles contributing to the estimation of the representative mean bending angle profile. Obviously, single bending angle profiles with values larger than  $\pm 50 \mu\text{rad}$  contribute to the estimate of the average bending angle profile (blue line). Furthermore the mean bending angle shows, dependent on altitude, a large standard deviation (green line). Performing the same analysis systematically on other zonal bins, presents large bending angle outliers contributing to the mean values of the single bins. Based on this result, we decided to perform an outlier rejection similar to the discussion in the ROM SAF report by Foelsche and Scherllin-Pirscher (2011). They decided to reject in an altitude range between 50 km to 80 km all bending angle profiles which are smaller than  $-40 \mu\text{rad}$  or larger than  $40 \mu\text{rad}$  to contribute to their BAROCLIM climatology (Bending Angle Radio Occultation Climatology). In this study we decided to reject an entire bending angle if single values of the profile are smaller or larger than  $\pm 30 \mu\text{rad}$  in the altitude region between 50 km and 80 km. To put this rejection criterion in a context, the global, climatological average bending angle at 50 km is about  $15 \mu\text{rad}$ . Usually we find for the CHAMP satellite, after applying the initial quality control used at the DMI, between about 4000 up to 5000 profiles per month. The additional bending angle quality control (QC) reduces this number of profiles per month for a value of about 100 up to 400 profiles.

The r.h.s. of Fig. 2 shows the result of the contributing single bending angle profiles when an additional outlier rejection has been applied, studying the same mean

## Average bending angle approach

J. Danzer et al.

Title Page

Abstract

Introduction

Conclusions

References

Tables

Figures



Back

Close

Full Screen / Esc

Printer-friendly Version

Interactive Discussion



**Average bending angle approach**

J. Danzer et al.

Title Page

Abstract

Introduction

Conclusions

References

Tables

Figures



Back

Close

Full Screen / Esc

Printer-friendly Version

Interactive Discussion



latitude bin as before. Obviously profiles with large variations are eliminated resulting in a smoother bending angle estimate and a smaller standard variation. Figure 1b shows for January 2007 the differences of the mean and median bending angle estimates relative to the co-located ECMWF reference profiles, for the case of an additionally applied QC. Clearly, rejecting the outliers removes large-scale wiggles in the mean bending angle climatology, while the median bending angles are almost unaffected by the new approach.

Gleisner and Healy (2013) used a combination of mean and median values to estimate the average bending angle values. Up to an altitude of 50 km they employed the mean bending angle, between the altitude range of 50 km to 60 km they performed a simple linear combination between mean and median, and above 60 km only the median bending angle was used. In this follow up study we also used a linear combination of mean and medians for averaged CHAMP bending angles. In an initial investigation we studied the relative differences of mean-median combinations to the co-located ECMWF reference profiles, using in a first attempt a transition region between 50 km to 60 km, comparing mean-median combinations where additional quality control was applied to combinations without additional quality control. For the case without extra QC some of the monthly mean-median bending angle estimates still exhibited sometimes large deviations from the smooth ECMWF reference profile, whereas averaged bending angles where prior an additional outlier rejection has been applied showed comparably small differences. Consequently this further encouraged the idea of applying an additional QC on the single bending angle profiles before calculating bending angle means.

Furthermore the sensitivity of employing different transition regions has been tested on the averaged bending angle profiles. Transition regions between 45 km to 55 km, 50 km to 60 km, and 55 km to 65 km, with and without outlier rejection have been analysed. Studying then the Abel processed averaged refractivity profiles, the results showed below altitudes of 45 km differences less than 0.1 % when comparing the transition regions. Hence, we decided to use a transition region between 50 km to

60 km for mean-median bending angle combination, as used previously with the COSMIC data.

## 4 CHAMP refractivity averages

Zonal monthly mean refractivity profiles were computed for CHAMP data using the new average-profile inversion as well as the standard single-profile inversion.

### 4.1 Initial analysis

In a first analysis the effect of applying an additional bending angle QC on monthly mean refractivity profiles was studied. To answer this question, monthly mean refractivity profiles have been calculated with and without additional QC, using the API technique. Figure 3 shows the relative difference between monthly mean refractivities, calculated with “Old QC” and with “New QC”, for CHAMP data from July 2007. “Old QC” refers to the standard QC at the DMI, applied on single profiles (Gorbunov et al., 2006), “New QC” refers to an additional outlier rejection at bending angle level. Differences between the two cases below an altitude of 30 km are less than  $|0.2|$  %, above 30 km areas of increased differences start to appear, showing for the case of July 2007 a value of up to 4 % at an altitude of 50 km. Investigating other months (not shown) the main impact of the additional QC is on the mid to high latitudes. To further extend the quality control investigation, API processed profiles with and without additional QC have been studied relative to co-located ECMWF profiles. In general profiles with additional QC showed smaller differences relative to co-located ECMWF profiles than when using only the standard quality control. This analysis together with the results of the bending angle study (see e.g., Fig. 1) lead to the decision always to apply an additional outlier rejection on bending angle profiles in the case of CHAMP data.

Next zonal monthly refractivities were compared, obtained from inverting averaged bending angles as well as statistically optimized single profiles. Figure 4 shows the

Title Page

Abstract

Introduction

Conclusions

References

Tables

Figures



Back

Close

Full Screen / Esc

Printer-friendly Version

Interactive Discussion



## Average bending angle approach

J. Danzer et al.

Title Page

Abstract

Introduction

Conclusions

References

Tables

Figures



Back

Close

Full Screen / Esc

Printer-friendly Version

Interactive Discussion



result of the difference between the two methods for the month November 2006, studying CHAMP data. The relative differences increase above an altitude of 40 km, reaching about  $\pm 5\%$  at 50 km altitude and high latitudes. As a next step, in Fig. 5 the relative difference between the inversion method and the co-located ECMWF profile was analyzed. The top plot shows the results for the new inversion technique, while the bottom plot shows the results for the standard inversion. Below 35 km differences with respect to ECMWF are almost identical for the two inversion methods. This shows that below 35 km statistical optimization did not cause any significant effects, due to the a priori information. Regarding the region between 35 km to 50 km differences start to increase relative to ECMWF with up to 5% at high latitudes, for the standard inversion. For the new inversion relative differences are smaller at high latitudes, compared to the standard retrieval. Figures 4 and 5 already hint to a known limitation of the current retrievals based on statistical optimization, showing larger biases during winter conditions at high latitudes and altitudes. The results suggest that through the introduction of the rather complex statistical optimization no obvious benefits are introduced in the generation of refractivity climatologies. Furthermore, performing a systematic analysis similar to Fig. 5 suggests that the API approach is feasible for both CHAMP and COSMIC data.

### 4.2 Detailed comparison of new inversion to standard inversion

One of the motivations for the introduction of the new retrieval scheme was to circumvent the rather complex SO, and hence removing a source of structural uncertainty from the processing. In Ao et al. (2012); Gleisner and Healy (2013) first positive results of the API technique, which is designed for the study of climatologies, were shown for COSMIC satellite data. However, it has been questioned if the API technique is also applicable to CHAMP data. The last section showed that average profile processing works for CHAMP data as well and long term trend studies are possible. However, it needs to be evaluated if the new retrieval scheme is equally good, or maybe even better, than the standard retrieval scheme. Hence, both processing methods need to be compared and studied on a longer time scale.



differences relative to ECMWF at high latitude winter months, but however also slightly larger differences in non-winter months. Further investigations will be necessary.

## 5 Discussion and conclusions

In this study the idea of forwarding bending angle climatologies, instead of SO single bending angle profiles, through an Abel transformation, was tested on CHAMP data. It has been shown that SO is a source of structural uncertainty between different processing centers (Steiner et al., 2013), which may be circumvented by averaging primarily in bending angle space. An initial analysis of the average bending angle approach has been performed on COSMIC satellite data (Ao et al., 2012; Gleisner and Healy, 2013). However, in order to obtain long-term climate data products the use of CHAMP data is also required. Since the CHAMP satellite mission has a reduced number of occultations compared to the COSMIC mission, and an increased noise level, it was questionable if the approach is also successful on CHAMP data.

The analysis was started by generating  $10^\circ$  monthly zonal bending angle profiles, studying bending angle means and medians. Due to large-scale wiggles in the mean value, an additional bending angle outlier rejection was introduced for values larger or smaller than  $\pm 30 \mu\text{rad}$  between an altitude of 50 km to 80 km.

After performing the Abel transformation on the average bending angle profiles, monthly zonal refractivities were studied, leading to the firm conclusion that the average bending angle approach is also applicable to CHAMP data. Below an altitude of 35 km the standard single profile processing and the average profile processing are almost identical, for CHAMP as well as for COSMIC satellite data. Above an altitude of 35 km differences between the two processing methods start to increase, showing largest differences at high altitudes and high latitudes.

In order to understand discrepancies better, and since it is known that retrievals based on SO may exhibit structural errors at high altitudes and high latitude winter conditions, a detailed analysis of this region was performed. Differences of monthly mean

## Average bending angle approach

J. Danzer et al.

Title Page

Abstract

Introduction

Conclusions

References

Tables

Figures



Back

Close

Full Screen / Esc

Printer-friendly Version

Interactive Discussion



**Average bending angle approach**

J. Danzer et al.

Title Page

Abstract

Introduction

Conclusions

References

Tables

Figures



Back

Close

Full Screen / Esc

Printer-friendly Version

Interactive Discussion



refractivities relative to co-located ECMWF data were studied on a longer time scale, detecting a clear signal of an increased bias relative to ECMWF at high latitudes in the winter time for the standard retrieval. For the new retrieval the bias was reduced, with however slightly larger deviations for non-winter months compared to the standard retrieval. The results of the average bending angle approach are still encouraging, since the agreement with ECMWF is slightly better. Studying mid to low latitudes the two retrievals showed practically identical results relative to ECMWF, indicating a robustness among the choice of the approach in that geographical region.

However, the slightly increased bias of the new approach relative to ECMWF data for non-winter months at high latitudes and the seasonal bias at mid to low latitudes, point to some remaining problems with the averaging approach. Further investigations will be necessary. For example, the impact of residual ionospheric errors needs to be investigated, since observational data is used up to higher altitudes. Although there is a general interest in handling this problem, in case of the averaging approach, the residual influence of the ionosphere needs to be understood. On the other hand, statistical optimization aims to reduce random errors, but by using a priori information it may partly mitigate that problem.

Nevertheless, for the application of climatologies the new approach showed some very promising results. Since up to 80 km altitude it is free of a priori information, the API technique makes the error characterisation of the resulting climate data products much easier. For the standard retrievals, used at different processing centers, it may be difficult to distinguish at what altitude the influence of the model data starts, and when purely observational data is used. This depends on the implementation of the SO of the processing center. Hence, as a next step it would be interesting to study the API technique with the retrieval of different processing centers and compare the resulting climate data products. If the differences are very small, it means that the new approach shows the encouraging result of a robustness among processing centers.

Finally, we also suggest to study spatial and temporal limits of the approach. So far 5° zonal bins on COSMIC data and 10° zonal bins on CHAMP and COSMIC data sets, on

## Average bending angle approach

J. Danzer et al.

Title Page

Abstract

Introduction

Conclusions

References

Tables

Figures

◀

▶

◀

▶

Back

Close

Full Screen / Esc

Printer-friendly Version

Interactive Discussion



a monthly basis, have been tested. It would be interesting to test a further longitudinal binning, e.g.,  $60^\circ \times 10^\circ$  longitudinal  $\times$  latitudinal bins, or testing a two week time scale on zonal bins. If the averaging approach starts to fail for other binning choices it means one is rather restricted to a fixed climatology.

We conclude that it is possible to retrieve monthly refractivity profiles directly from averaged bending angles, using RO data from the CHAMP satellite mission. At that point the investigations showed very positive results which opened the door to a valid way of circumventing the SO step in climatological studies. Further necessary investigations have been pointed out and discussed, which should clarify limits and possibilities of the new approach.

*Acknowledgements.* We thank UCAR/CDACC for providing CHAMP and COSMIC excess phase data, and the ECMWF for providing analysis data. Furthermore we are grateful to ROM SAF, which made the visiting scientist activity possible, under which the work was conducted. Finally we thank Kent B. Lauritsen at the DMI for discussions and his support, and at the WEGC Marc Schwärz for his technical support.

## References

- Ao, C. O., Mannucci, A. J., and Kursinski, E. R.: Improving GPS radio occultation stratospheric refractivity retrievals for climate benchmarking, *Geophys. Res. Lett.*, 39, L12701, doi:10.1029/2012GL051720, 2012. 7814, 7818, 7822, 7824
- Foelsche, U. and Scherllin-Pirscher, B.: Development of bending angle climatology from RO data, Tech. rep., GRAS-SAF, 2011. 7815, 7819
- Foelsche, U., Kirchengast, G., Steiner, A. K., Kornblueh, L., Manzini, E., and Bengtsson, L.: An observing system simulation experiment for climate monitoring with GNSS radio occultation data: setup and test bed study, *J. Geophys. Res.*, 113, D11108, doi:10.1029/2007JD009231, 2008. 7817
- Gleisner, H. and Healy, S. B.: A simplified approach for generating GNSS radio occultation refractivity climatologies, *Atmos. Meas. Tech.*, 6, 121–129, doi:10.5194/amt-6-121-2013, 2013. 7814, 7815, 7818, 7820, 7822, 7824

## Average bending angle approach

J. Danzer et al.

Title Page

Abstract

Introduction

Conclusions

References

Tables

Figures



Back

Close

Full Screen / Esc

Printer-friendly Version

Interactive Discussion



Gobiet, A. and Kirchengast, G.: Advancements of Global Navigation Satellite System radio occultation retrieval in the upper stratosphere for optimal climate monitoring utility, *J. Geophys. Res.*, 109, D24110, doi:10.1029/2004JD005117, 2004. 7814, 7817

Gorbunov, M.: Canonical transform method for processing radio occultation data in the lower troposphere, *Radio Sci.*, 37, 1076, doi:10.1029/2000RS002592, 2002. 7814, 7817

Gorbunov, M., Lauritsen, K., Rhodin, A., Tomassini, M., and Kornblueh, L.: Radio holographic filtering, error estimation, and quality control of radio occultation data, *J. Geophys. Res.*, 111, D10105, doi:10.1029/2005JD006427, 2006. 7816, 7819, 7821

Ho, S.-P., Kirchengast, G., Leroy, S., Wickert, J., Mannucci, A. J., Steiner, A. K., Hunt, D., Schreiner, W., Sokolovskiy, S., Ao, C., Borsche, M., von Engel, A., Foelsche, U., Heise, S., Iijima, B., Kuo, Y.-H., Kursinski, E. R., Pirscher, B., Ringer, M., Rocken, C., and Schmidt, T.: Estimating the uncertainty of using GPS radio occultation data for climate monitoring: intercomparison of CHAMP refractivity climate records from 2002 to 2006 from different data centers, *J. Geophys. Res.*, 114, D23107, doi:10.1029/2009JD011969, 2009. 7814

Ho, S.-P., Hunt, D., Steiner, A. K., Mannucci, A. J., Kirchengast, G., Gleisner, H., Heise, S., von Engel, A., Marquardt, C., Sokolovskiy, S., Schreiner, W., Scherllin-Pirscher, B., Ao, C., Wickert, J., Syndergaard, S., Lauritsen, K. B., Leroy, S., Kursinski, E. R., Kuo, Y.-H., Foelsche, U., Schmidt, T., and Gorbunov, M.: Reproducibility of GPS radio occultation data for climate monitoring: profile-to-profile inter-comparison of CHAMP climate records 2002 to 2008 from six data centers, *J. Geophys. Res.*, 117, D18111, doi:10.1029/2012JD017665, 2012. 7814, 7817

Kursinski, E. R., Hajj, G. A., Schofield, J. T., Linfield, R. P., and Hardy, K. R.: Observing Earth's atmosphere with radio occultation measurements using the Global Positioning System, *J. Geophys. Res.*, 102, 23429–23465, doi:10.1029/97JD01569, 1997. 7816, 7817

Lauritsen, K. B., Syndergaard, S., Gleisner, H., Gorbunov, M. E., Rubek, F., Sørensen, M. B., and Wilhelmsen, H.: Processing and validation of refractivity from GRAS radio occultation data, *Atmos. Meas. Tech.*, 4, 2065–2071, doi:10.5194/amt-4-2065-2011, 2011. 7814

Lohmann, M. S.: Application of dynamical error estimation for statistical optimization of radio occultation bending angles, *Radio Sci.*, 40, RS3011, doi:10.1029/2004RS003117, 2005. 7814

Scherllin-Pirscher, B.: Further development of BAROCLIM and implementation in ROPP, Tech. rep., GRAS-SAF, 2013. 7815

Steiner, A. K., Hunt, D., Ho, S.-P., Kirchengast, G., Mannucci, A. J., Scherllin-Pirscher, B., Gleisner, H., von Engeln, A., Schmidt, T., Ao, C., Leroy, S. S., Kursinski, E. R., Foelsche, U., Gorbunov, M., Heise, S., Kuo, Y.-H., Lauritsen, K. B., Marquardt, C., Rocken, C., Schreiner, W., Sokolovskiy, S., Syndergaard, S., and Wickert, J.: Quantification of structural uncertainty in climate data records from GPS radio occultation, *Atmos. Chem. Phys.*, 13, 1469–1484, doi:10.5194/acp-13-1469-2013, 2013. 7814, 7815, 7817, 7824

5

## AMTD

7, 7811–7835, 2014

### Average bending angle approach

J. Danzer et al.

Title Page

Abstract

Introduction

Conclusions

References

Tables

Figures



Back

Close

Full Screen / Esc

Printer-friendly Version

Interactive Discussion



## Average bending angle approach

J. Danzer et al.

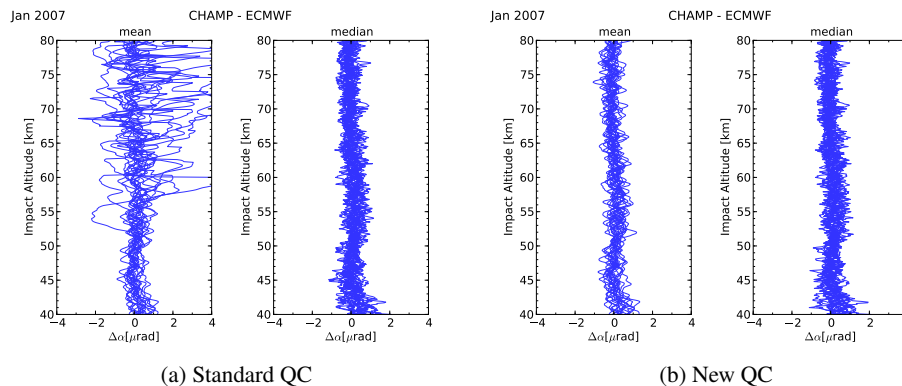


**Figure 1.** Difference between observed bending angle means and medians to co-located ECMWF analysis data, comparing the results with standard QC to the results where an additional bending angle QC has been applied.

[Title Page](#)[Abstract](#)[Introduction](#)[Conclusions](#)[References](#)[Tables](#)[Figures](#)[◀](#)[▶](#)[◀](#)[▶](#)[Back](#)[Close](#)[Full Screen / Esc](#)[Printer-friendly Version](#)[Interactive Discussion](#)

## Average bending angle approach

J. Danzer et al.

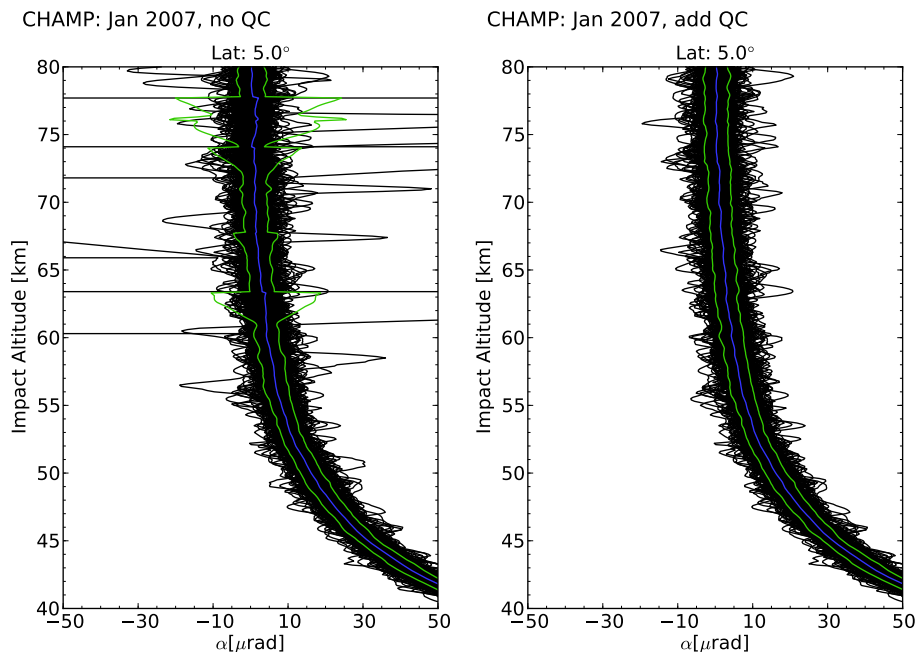


**Figure 2.** The l.h.s. plot shows all observational bending angle profiles for the northern fundamental bin at mean latitude 5°, while the r.h.s. shows the same, but outliers  $\pm 30 \mu\text{rad}$  have been rejected. The blue line represents the mean value of all profiles for each bin, the green line its standard deviation.

[Title Page](#)[Abstract](#)[Introduction](#)[Conclusions](#)[References](#)[Tables](#)[Figures](#)[◀](#)[▶](#)[◀](#)[▶](#)[Back](#)[Close](#)[Full Screen / Esc](#)[Printer-friendly Version](#)[Interactive Discussion](#)

## Average bending angle approach

J. Danzer et al.

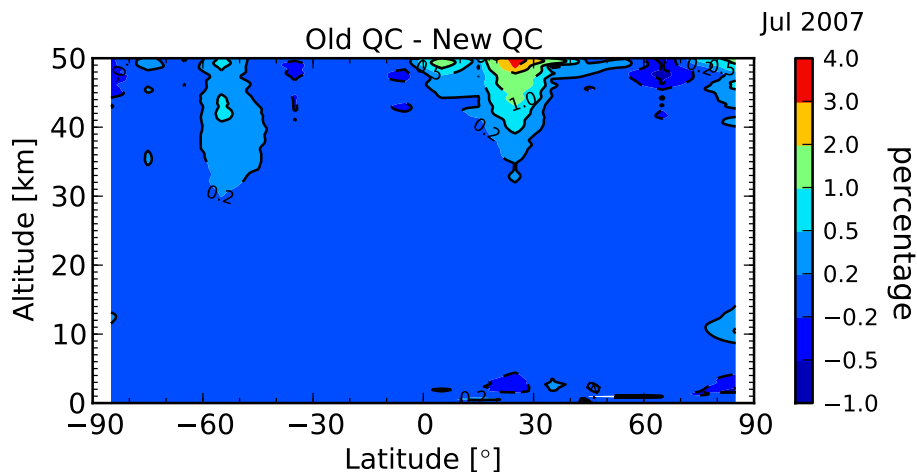


**Figure 3.** Relative difference between monthly mean refractivities obtained by average-profile inversion with standard quality control (Old QC) and additional quality control (New QC), for CHAMP data from July 2007.

[Title Page](#)[Abstract](#)[Introduction](#)[Conclusions](#)[References](#)[Tables](#)[Figures](#)[◀](#)[▶](#)[◀](#)[▶](#)[Back](#)[Close](#)[Full Screen / Esc](#)[Printer-friendly Version](#)[Interactive Discussion](#)

Refractivity Difference

Nov 2006

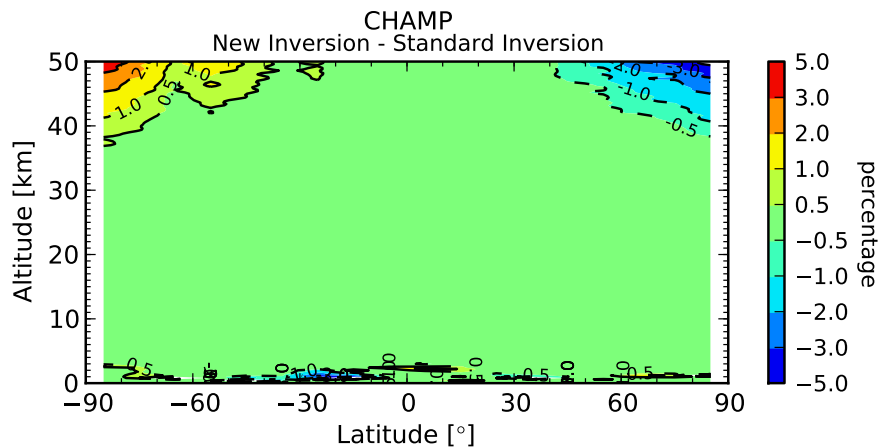


**Figure 4.** Relative difference between monthly mean refractivity from CHAMP data, using average-profile inversion and standard inversion, for November 2006.

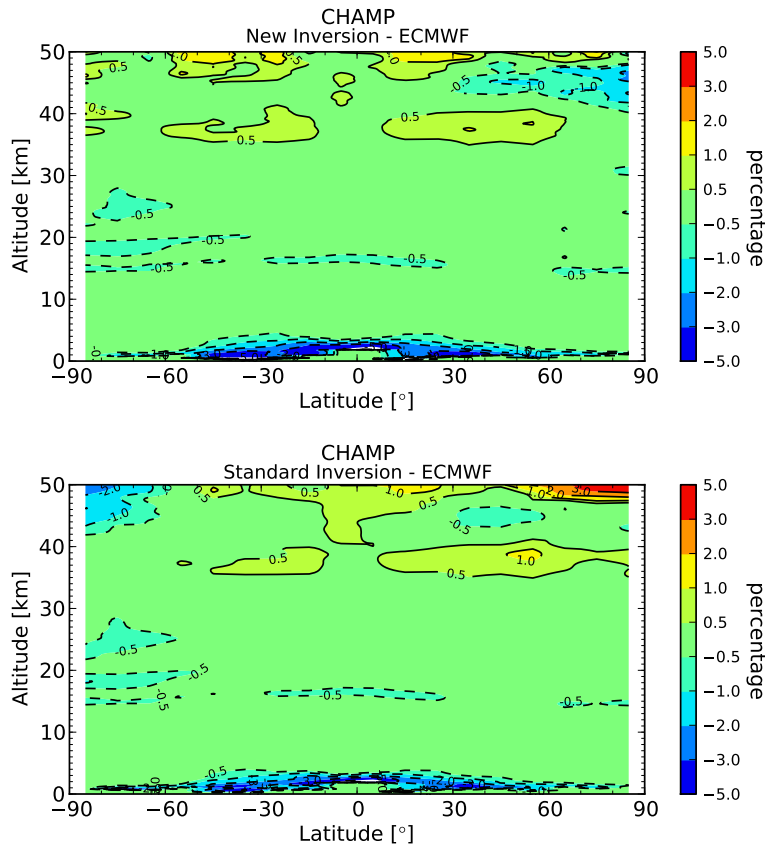


**Figure 5.** Relative difference between monthly mean refractivity from CHAMP data and from collocated ECMWF data, using average-profile inversion (top plot) and standard inversion (bottom plot), for November 2007.

Title Page

Abstract

Introduction

Conclusions

References

Tables

Figures



Back

Close

Full Screen / Esc

Printer-friendly Version

Interactive Discussion



## Average bending angle approach

J. Danzer et al.

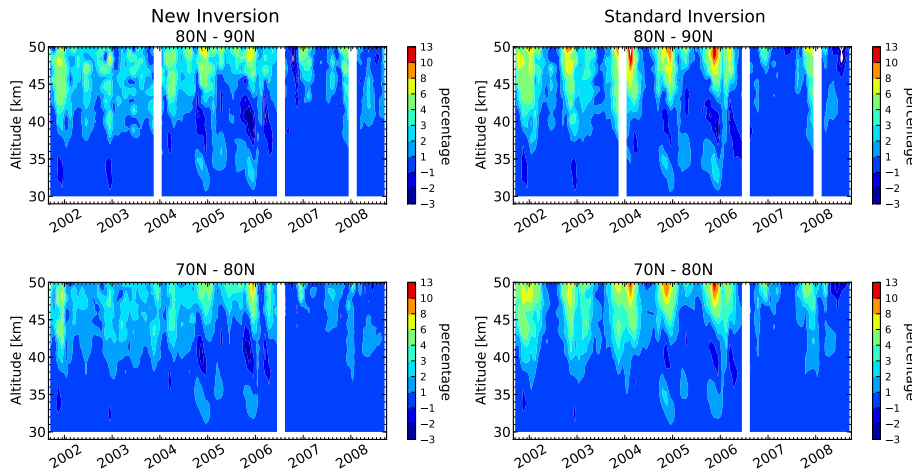


**Figure 6.** Relative differences between monthly mean refractivities from CHAMP data and from collocated ECMWF data, comparing new inversion (l.h.s.) and standard inversion (r.h.s.), from September 2001 until September 2008 for the zonal bins  $80^{\circ}$  N to  $90^{\circ}$  N and  $70^{\circ}$  N to  $80^{\circ}$  N.

[Title Page](#)[Abstract](#)[Introduction](#)[Conclusions](#)[References](#)[Tables](#)[Figures](#)[◀](#)[▶](#)[◀](#)[▶](#)[Back](#)[Close](#)[Full Screen / Esc](#)[Printer-friendly Version](#)[Interactive Discussion](#)

## Average bending angle approach

J. Danzer et al.

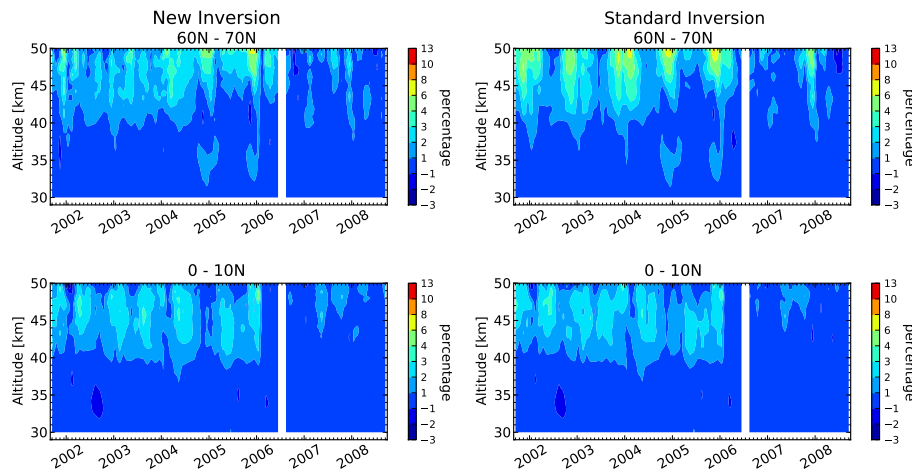


**Figure 7.** Relative differences between monthly mean refractivities from CHAMP data and from collocated ECMWF data, comparing new inversion (l.h.s.) and standard inversion (r.h.s.), for September 2001 until September 2008 and  $10^\circ$  zonal bins for northern mid to low latitudes.

Title Page

Abstract

Introduction

Conclusions

References

Tables

Figures



Back

Close

Full Screen / Esc

Printer-friendly Version

Interactive Discussion

